Submitted for publication in ApJ Letters
Preprint typeset using LATEX style emulateapj v. 12/16/11

THE KINEMATICS OF THE LOCAL GROUP IN A COSMOLOGICAL CONTEXT

J. E. Forero-Romero[1], Y. Hoffman[2], S. Bustamante[3], S. Gottlöber[4], G. Yepes[5]

(Dated: February 11, 2013)
Submitted for publication in ApJ Letters

ABSTRACT

Recent observations constrained the tangential velocity of M31 with respect to the Milky Way (MW) to be $v_{\rm M31,tan} < 34.4$ km s^{-1}and the radial velocity to be in the range $v_{\rm M31,rad} = -109 \pm 4.4$ km s^{-1}(van der Marel et al. 2012). In this study we use a large volume high resolution N-body cosmologicalsimulation (BOLSHOI) to statistically study this kinematics in the context of the ΛCDM cosmology and three constrained simulations designed to reproduce the Local Group (LG) and the local cosmic neighborhood. A LG is defined here as composed by two dominant separate halos hosting the MW and the M31 galaxy fulfilling certain isolation criteria. An ensemble of all BOLSHOI pairs fulfilling this selection is constructed, and also a subsample of it which obeys more stringent observational constraints on the mass and separation of of the MW and M31. The comparison of the ensembles of simulated pairs with the observed LG has been done with respect to the observed radial and tangential, the reduced orbital energy (e) and angular momentum (l) of the LG, and with respect to the dimensionless spin parameter, λ. Our main results are: (i) the prefered radial and tangential velocities for pairs in ΛCDM are $v_{\rm r} = -80 \pm 20$, $v_{\rm t} = 50 \pm 10$, (ii) pairs around that region are 3 to 13 times more common than pairs within the observational values, (iii) 15% to 24% of pairs in ΛCDM have energy and angular momentum consistent with observations while (iv) 9% to 13% of pairs in the same sample show similar values to the inferred dimensionless spin parameter. It follows that the quasi-conserved quantities quantities that characterize the orbit of the LG, i.e. e, l and λ, do not challenge the standard ΛCDM model, but that model is in tension with regard to the particular phase on the orbit of the LG, namely the actual values of the radial and tangential velocities. This might hint to a problem of the ΛCDM model to reproduce the observed LG.

Subject headings: galaxies: kinematics and dynamics, Local Group, methods:numerical

1. INTRODUCTION

The Milky Way (MW) and Andromeda galaxy (M31) are the dominant galaxies in the Local Group (LG). Astronomical observations of their mass distribution impose constraints on the standard cosmological model. The satellite overabundance problem (Klypin et al. 1999b; Moore et al. 1999), tidal disruption features (McConnachie et al. 2009) and the disk dominated morphology (Kazantzidis et al. 2008) are examples on of how LG studies are linked to the cosmological context. Detailed studies on the Magellanic Clouds dynamics and their possible link to M31 add to the interest of understanding the details of the LG kinematics and dynamics (Besla et al. 2007; Tollerud et al. 2011; Knebe et al. 2011; Fouquet et al. 2012; Teyssier et al. 2012). However, a general concern in the use of the LG as a tool for near-field cosmology (Freeman & Bland-Hawthorn 2002; Peebles & Nusser 2010) is how typical is the LG regarding the properties of interest (Busha et al. 2011; Liu et al. 2011; Forero-Romero et al. 2011; Purcell & Zentner 2012).

A new valuable piece of information in this issue is the recent observational determination of the proper-motion measurements of M31, which until recently had been out of reach (van der Marel et al. 2012). The reported measurements set an upper bound for the tangential velocity of M31 with respect to the MW of $v_{\rm tan,M31} \leq 34.4$ km s^{-1}. Together with the values of the relative radial velocity of $v_{\rm rad,M31} = -109 \pm 4.4$ km s^{-1}observations show that the relative motion of the MW and Andromeda is consistent with a head-on collision. With this information it is possible to quantify how common is this kinematic configuration in a ΛCDM Universe.

This Ltter presents such study. We use a large volume, high resolution dark matter only N-body simulation in the concordance ΛCDM cosmology to find a set of halo pairs with similar characteristics as inferred in the LG. We quantify these results in terms of the number of pairs with given radial and tangential velocities in the galactocentric rest frame. We also find the pairs that are consistent with a head on collision in terms of the ratio of the radial to tangential velocity $f_{\rm t} \equiv v_{\rm tan}/v_{\rm rad} < 0.3$ and present these results in terms of the reduced angular momentum and mechanical energy.

In addition we make use of three constrained N-body simulations which are constructed to reproduce the observed large scale structure of the Local Universe on scales of a few tens of Mpc. The special feature of these simulations is that each volume features a pair of halos with the right characteristics to be considered LG-like objects.

This Letter is structured as follows. In the next section we present the N-body simulations, the criteria we

[1] Departamento de Física, Universidad de los Andes, Cra. 1 No. 18A-10, Edificio Ip, Bogotá, Colombia, je.forero@uniandes.edu.co
[2] Racah Institute of Physics, The Hebrew University of Jerusalem, 91904 Jerusalem, Israel
[3] Instituto de Física - FCEN, Universidad de Antioquia, Calle 67 No. 53-108, Medellín, Colombia
[4] Leibniz-Institut für Astrophysik, Potsdam, An der Sternwarte 16, 14482 Potsdam, Germany
[5] Grupo de Astrofísica, Departamento de Física Teórica, Universidad Autónoma de Madrid, Cantoblanco E-280049, Spain

use to select LG-like halo pairs. In Section 3 we present the results for the dynamics in these pairs in terms of the tangential/radial velocities and the orbital angular momentum/mechanical energy. In the same section we sumarize these dynamical results in terms of the dimensionless spin parameter of the pairs. Finally, in the last section we comment and conclude about the implications of these results in the context of the ΛCDM model.

2. SIMULATION AND ENVIRONMENT

2.1. *The Bolshoi and Constrained Simulations*

The Bolshoi simulation follows the non-linear evolution of the dark matter density field using N-body techniques. The simulation has a cubic volume of $250h^{-1}$Mpc comoving on a side, sampled with 2048^3 particles. The cosmological parameters used in the simulation are $\Omega_m = 0.27, \Omega_\Lambda = 0.73, \sigma_8 = 0.82, h = 0.70$ and $n = 0.95$, corresponding to the matter density, vacuum energy density, the normalization of the power spectrum, the dimensionless Hubble constant and the index of the slope in the initial power spectrum. This set of parameters is compatible with the analysis of the seventh year of data from the Wilkinson Microwave Anisotropy Probe (WMAP) (Jarosik et al. 2011). A detailed description of this simulation can be found in (Klypin et al. 2011).

With these parameters the mass per particle is $m_p = 1.4 \times 10^8 h^{-1}\mathrm{M}_\odot$. In this paper we use algorithms obtained through the Bound Density Maxima (BDM) algorithm (Klypin et al. 1999a). The halos are selected to have an overdensity of 200 times the critical density. Furthermore, we only include in the analysis haloes whose center is located outside the virial radius of any other halo. We have obtained the data through the public available Multidark database [6] (Riebe et al. 2011). The database allows us to obtain the comoving positions, peculiar velocities and masses for all the halos in the simulation volume at $z = 0$. The positions and velocities of these haloes correspond to the average values of the 250 most bound particles. The Hubble flow is taken into account to convert the peculiar velocities into physical velocities and allow for a comparison with observations. We have verified that the main conclusions of this paper hold in the case of halos defined by a FOF algorithm with a linking lentgth 0.17 times the interparticle distance.

The constrained simulations we use in this Letter are part of the Constrained Local UniversE Simulations (CLUES) project whose main objective is to reproduce the large scale structure in the Local Universe as accurately as possible. The algorithm and observational constraints to construct the initial conditions are described in (Gottloeber et al. 2010). We use three dark matter only simulations, each has a cubic volume of $64h^{-1}$Mpc on a side, with the density field sampled with 1024^3 particles. The cosmological density parameter is $\Omega_m = 0.28$, the cosmological constant $\Omega_\Lambda = 0.72$, the dimensionless Hubble parameter $h = 0.73$, the spectral index of the primordial density perturbations $n = 0.96$ and the power spectrum normalization $\sigma_8 = 0.817$, also consistent with WMAP 7th year data.

2.2. *The LG-sample*

Based on the BDM catalogs in the Bolshoi simulation we construct a halo pair sample with the dynamical properties consistent with those of the MW and M31. The criteria we impose to define a LG-like halo pair are the following:

1. Each halo has a mass in the range $5\times10^{11}h^{-1}\mathrm{M}_\odot < M_h < 5 \times 10^{12}h^{-1}\mathrm{M}_\odot$.

2. With respect to each halo, there cannot be any other halo within the mass range $5\times10^{11}h^{-1}\mathrm{M}_\odot < M_h < 5 \times 10^{12}h^{-1}\mathrm{M}_\odot$ closer than its partner. It means that there cannot be ambiguity on the identity of the pair members.

3. The relative radial velocity between the two halos is negative (van der Marel et al. 2012).

4. The distance between the center of mass of the halos must be less than $0.7h^{-1}$Mpc (Ribas et al. 2005; van der Marel & Guhathakurta 2008).

5. There cannot be halos more massive than $5 \times 10^{12}h^{-1}\mathrm{M}_\odot$within a radius of $2h^{-1}$Mpc with respect to every object centre (Karachentsev et al. 2004; Tikhonov & Klypin 2009).

6. There cannot be halos more massive than $5 \times 10^{13}h^{-1}\mathrm{M}_\odot$within a radius of $3h^{-1}$Mpc with respect to every object centre (Karachentsev et al. 2004).

This sample in the Bolshoi simulation has 1923 pairs. Additionally, there is a sample of three (3) pairs constructed from the three constrained realizations. These pairs fulfill all the above mentioned conditions and additionally are located in a place with the right distances with respect to the Virgo cluster in the simulation. Figure 1 show the distribution of separations and total pair mass computed from the 1923 pairs in the Bolshoi simulation.

The full observational characteristics that we take in this Letter for the MW-M31 pair are listed in Table 1. A more restrictive subsample of LG-like objects has been constructed so as to fit obey the observational bounds on the masses and separation of the two main halos. These amount to:

1. The separation between the center of mass of the halos is in the range $700 - 800$kpc (Ribas et al. 2005; van der Marel & Guhathakurta 2008).

2. The total mass of the two halos is in the range $1 - 4 \times 10^{12}\mathrm{M}_\odot$(van der Marel et al. 2012).

Including these conditions the full pair sample is reduced from 1923 to 158 pairs. Note that only one constrained LG-like object is included in the subsample.

3. RESULTS

3.1. *Radial and tangential velocities*

Figure 2 summarizes the central finding of this Letter. Most of the pairs in the two samples constructed from the Bolshoi Simulation have radial and tangential velocities notably different from the observational constraints.

[6] http://www.multidark.org/MultiDark/

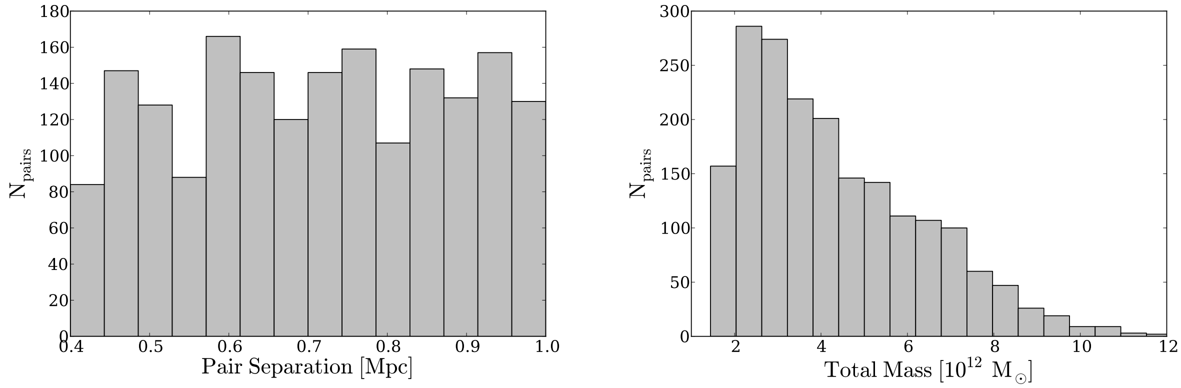

FIG. 1.— Distributions of separations and total halo mass (Milky Way and M31) in the LG-like pairs selected from the Bolshoi Simulation.

TABLE 1
SUMMARY OF OBSERVATIONAL CONSTRAINTS. THE KINEMATIC PROPERTIES FOR M31 ARE REPORTED IN THE GALACTOCENTRIC (VAN DER MAREL ET AL. 2012). VALUES IN PARENTHESIS CORRESPOND TO VECTOR COMPONENTS. $\sigma_{\mathbf{x}}$ REPRESENTS THE UNCERTAINTY ON THE COMPONENTS OF VECTOR $\mathbf{x}$. THE VALUES FOR THE INDIVIDUAL HALO MASSES ARE CONSISTENT WITH THE PRIORS USED BY VAN DER MAREL ET AL. (2012).

$v_{\rm M31,rad}$	(km s^{-1})	-109.3 ± 4.4
$v_{\rm M31,tan}$	(km s^{-1})	< 34.4
$r_{\rm M31}$	(kpc)	770 ± 40
$\mathbf{r}_{\rm M31}$	(kpc)	$(-378.9, 612.7, -283.1)$
$\sigma_{\mathbf{r},\rm M31}$	(kpc)	$(-18.9, 30.6, 14.5)$
$\mathbf{v}_{\rm M31}$	(km s^{-1})	$(66.1, -76.3, 45.1)$
$\sigma_{\mathbf{v},\rm M31}$	(km s^{-1})	$(26.7, 19.0, 26.5)$
$M_{200,\rm MW}$	(10^{12}M$_\odot$)	1.6 ± 0.5
$M_{200,\rm M31}$	(10^{12}M$_\odot$)	1.6 ± 0.5
$M_{200,\rm MW} + M_{200,\rm M31}$	(10^{12}M$_\odot$)	3.14 ± 0.58
$\log_{10}\lambda$		-1.72 ± 0.07

Note: the observational uncertainties in the position vector correspond to a 5% in each component consistent with the uncertainties in the distance (see references in van der Marel & Guhathakurta 2008). Note: the value for $\log_{10}\lambda$ is obtained in this Letter from a Monte Carlo simulation as described in Section XX.

TABLE 2
SUMMARY OF RESULTS FROM ΛCDM.

		Full Sample	Reduced Sample
$v_{\rm M31,rad}$	(km s^{-1})	-70 ± 10	-90 ± 10
$v_{\rm M31,tan}$	(km s^{-1})	50 ± 10	50 ± 10
$\log_{10}\lambda$		-1.47 ± 0.13	-1.34 ± 0.12

Note: the observational uncertainties in the position vector correspond to a 5% in each component consistent with the uncertainties in the distance (see references in van der Marel & Guhathakurta 2008)

The most probable radial and tangential velocities in ΛCDM are summarized in Table 2. For the full sample we have $v_{\rm rad,\Lambda CDM} = -70 \pm 10\,{\rm km\ s^{-1}}$and $v_{\rm tan,\Lambda CDM} = 50 \pm 20$ km s^{-1}. For the reduced sample $v_{\rm rad,\Lambda CDM} = -90 \pm 10\,{\rm km\ s^{-1}}$and $v_{\rm tan,\Lambda CDM} = 50 \pm 20$ km s^{-1}, where the uncertainties in these values reflect the minimum grid size needed to obtain robust statistics for the 2D histogram.

The number of pairs withing the range of uncertainty of observations are listed in Table 3 (columns 2 and 3). In the same table (columns 4 and 5) we summarize the number of pairs around the ΛCDM values within the same range of absolute observational uncertainty (i.e. $\sigma_{\rm tan} = 17\,{\rm km\ s^{-1}}$and $\sigma_{\rm rad} = 4\,{\rm km\ s^{-1}}$.)

From these results we infer that the pairs around the preferred phase space for ΛCDM are at least 13 times more common than pairs with the observed velocities for the Local group. We highlight that this is a lower bound given that in the reduced sample none of the pairs are found in the interval allowed by observations. The high eccentric orbit of the observed LG constitutes an unlikely configurations for the ΛCDM LG-like objects. This holds for the full and the subsample of objects.

From Figure 2 it is also clear that there is a significant number of pairs with a high tangential-to-radial velocity ratio. The peak in the pair number density is located around a region of $f_{\rm t} \equiv v_{\rm tan\Lambda CDM}/v_{\rm rad\Lambda CDM} \sim 0.7$, while the observations suggest $f_{\rm t} < 0.32$. As summarized in Table 3 we find that only between 8% to 12% of the pairs are consistent with the observational constraint. The three pairs from the constrained realizations are also outside the region of the most probable values in a ΛCDM cosmology with tangential-to-radial ratios of $f_{\rm t} = 0.35, 0.45, 0.73$.

3.2. *Reduced Angular Momentum and Energy*

The two-body problem of point-like masses can serve as a proxy for the dynamics of the LG and be used as a tool for studying the LG within the framework of the standard cosmological model. Within the model the dynamics of the LG is governed by the (center of mass) reduced angular momentum $l = \mathbf{r}_{\rm M31} \times \mathbf{v}_{\rm M31}|$ and reduced energy $e = \frac{1}{2}\mathbf{v}_{\rm M31}|^2 - GM/|\mathbf{r}_{\rm M31}|$, where the total mass is $M = m_{\rm M31} + m_{\rm MW}$, the reduced mass is $\mu = m_{\rm M31}m_{\rm MW}/M$ and G is the gravitational constant.

This formulation has a clear theoretical advantage if one considers the angular momentum and the mechanical energy as quasi-conserved dynamical quantities. This means that, after some formation time, these quantities do not significantly evolve as it is the case for the radial and tangential velocities.

However, this formulation has an observational disadvantage. The reduced energy and angular momentum are derived from very different kinds of observations, in-

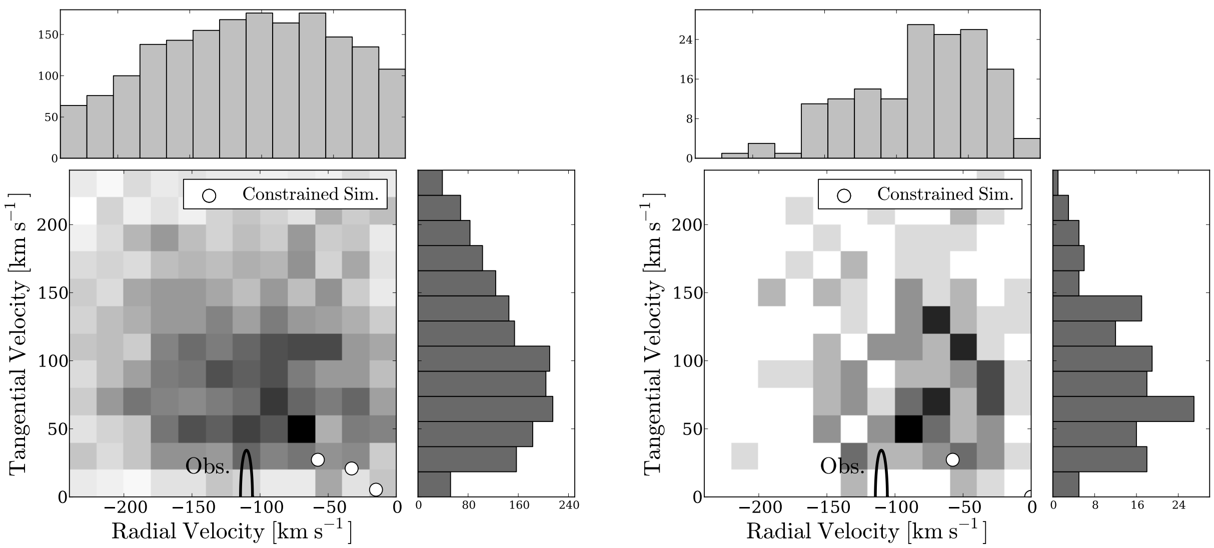

FIG. 2.— Histograms of the radial and tangential velocities for LG-like halo pairs in the Bolshoi simulation. The left (right) panel correspond to the full (reduced) pair sample. The squared panel shows as a shaded histogram the number of pairs on the radial and tangential velocities plane. The rectangular panels show the histograms when only one of the velocity components is used to bin the data. The half ellipse corresponds to the observed observational and the circles represent the positions of the pairs from the constrained simulations. The locii for the highest density regions are listed in Table 2.

TABLE 3
SUMMARY OF THE COMPARISON OF THE OBSERVATIONAL RESULTS AGAINST ΛCDM.

Physical property	(%) Pairs consistent with observations in full sample	% Pairs consistent with observations in reduced sample	% Pairs consistent with ΛCDM in full sample	(%) Pairs consistent with ΛCDM in reduced sample
$v_{\rm r}$-$v_{\rm t}$	(0.4%) 8/1923	(0%)0/158	(1%)23/1923	(8%)13/158
$e_{\rm tot}$-$l_{\rm orb}$	(15%)298/1923	(24%)38/158	-	-
$\log_{10}\lambda$	(13%)257/1923	(9%)15/158	-	-
$r_{\rm t}=v_{\rm t}/v_{\rm r}$	(12%)242/1923	(8%)13/158	-	-

Note: In columns 4 and 5 the number of pairs around the prefered region in $v_{\rm r}-v_{\rm t}$ in ΛCDM (as shown in Fig. **??** and summarized in Table 2) are calculated within the same observational absolute uncertainty.

creasing the uncertainties in their final determination.

A possible conflict between the likelihood of the LG in the ΛCDM model as viewed from the radial and tangential velocities as opposed to the angular momentum and energy perspectives would point to a particular phase on the LG two-body orbit. Given the masses, velocity and position of the observed MW and M31 (Table 1) the reduced energy and angular momentum are calculated. The Monte Carlo sampling is used to to estimate the uncertainty in these quantities.

Figure 3 presents the reduced energy and angular momentum distribution of the constrained and unconstrained LG-like objects of the full and subsample, following the plotting conventions from Figure 2. The 1-σ contour of Figure 3 does not cross the zero level, as can be naively expected from Figure 2. This happens for the $\approx 80\%$ level contour. The small difference between the presentations of the observational uncertainties in Figure 2 versus Figure 3 stems from the Monte Carlo sampling.

Visual inspection of Figure 3 shows that the $e_{\rm tot}$ and $l_{\rm orb}$ constraints are less restrictive compared with the radial and tangential velocity constraints. As summarize in Table 3, for the unconstrained full (sub-) sample 15% (24%) of the LG-like pairs obey the 1-σ observational constraints.

All the constrained LGs of the full samples are consistent with the 1-σ observationaluncertainty. However a reduction by a factor of 2 in the uncertainty of the tangential velocity showing that the tangential velocity is below 17 km s^{-1}would bring these pairs and the ΛCDM expectation outside the 1-σ observational uncertainty.

3.3. *Dimensionless Spin Parameter*

The dimensionless spin parameter λ (Peebles 1971) is used here to characterize the dynamical state of the observed and simulated LGs. The parameter measures the dynamical role of the angular momentum in terms of the gravitational attraction and is defined by

$$\lambda = \frac{\mu^{3/2} l_{\rm orb}\sqrt{e_{\rm tot}}}{GM^{5/2}}, \qquad (1)$$

where the $\mu = m_{\rm M31}m_{\rm MW}/M$ is the reduced mass for the pair.

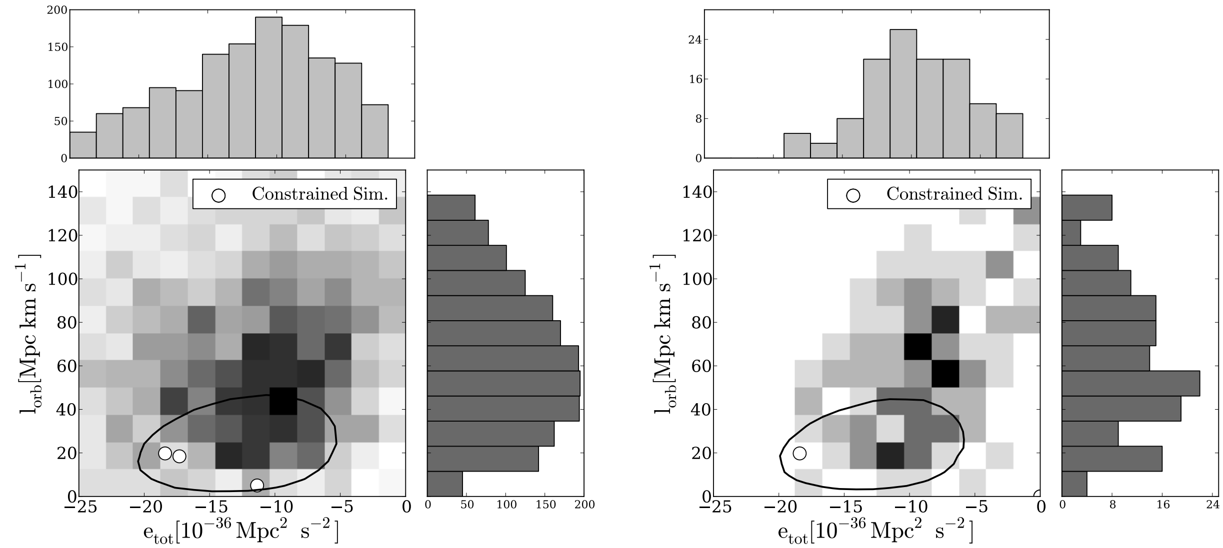

FIG. 3.— Histograms of the orbital angular momentum ($l_{\rm orb}$) and mechanical energy ($e_{\rm tot}$) per unit of reduced mass calculated considering the halos as point masses. The panel distribution is the same as in Figure 2. The contour line encloses 68% of the Monte Carlo generated points to estimated the uncertainties from the observational values summarized in Table 1. The constraints in this plot are less restrictive than in Fig.2 due to added uncertainties on the tangential velocity (100%), the square of the norm of the velocity (40%) and the total mass of the two halos (20%).

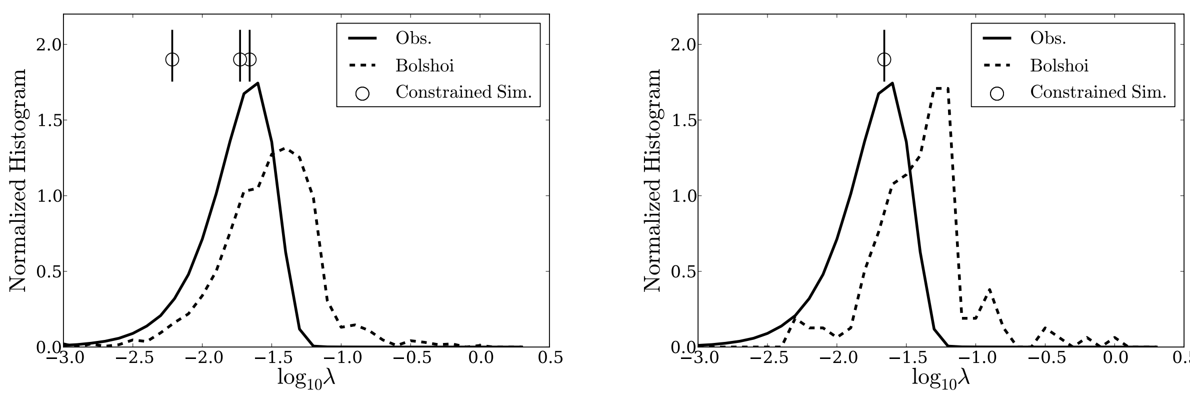

FIG. 4.— Normalized histograms of Peeble's spin parameter λ for the pairs in the Bolshoi simulation and its infered values for the LG from the observational constraints from a Monte Carlo simulation. The left (right) panel corresponds to the full (reduced) sample. The vertical lines with the white dots represent the values inferred for pairs in the constrained simulations.

We compare the distribution for λ obtained from the pair population in the Bolshoi simulation and the distribution from the Monte Carlo simulation used to estimate the uncertainties on $e_{\rm tot}$ and $l_{\rm orb}$. Figure 4 shows the likelihood distribution of the observational errors and the spin parameter of the LG-like pairs of the full (left panel) and the sub- (right panel) samples. The value of λ of the constrained LGs is shown as well.

The expected configuration in energy and angular momentum of the LG is slightly inconsistent with the expectation from halo pairs in ΛCDM.

The spin parameter of the simulated LG-like objects is skewed towards higher values compared with the observationally estimated value. Inspection of Figure 4 shows that the λ distribution is close to a lognormal one and thus resembles the distribution of the spin parameter of DM halos in simulation (**Jaime - please provide a reference**) . The estimated value of $\log_{10}\lambda$ of the observed LG is -1.76, compared with the mean value of $\log_{10}\lambda$ of -1.51 for the full sample and -1.38 for the subsample. The values of the spin parameter of the 3 constrained LGs are $\log_{10}(\lambda_{\rm CLUES}) = -2.21$, -1.72 and -1.65, with the latter value belonging to the sole constrained LG of the subsample.

It follows that the observationally estimated energy and angular momentum and the estimated spin parameter impose similar constraints on the simulations and the standard model of cosmology.

4. CONCLUSIONS

We have presented a comparison between the observed kinematics for the M31 in the galactocentric restframe and the expectations for a large N-body cosmological simulation in the ΛCDM cosmology. In the simulation we select a sample of halo pairs in the mass range $5 \times 10^{11} < M_h/h^{-1}\mathrm{M}_\odot < 5 \times 10^{12}$ that closely match the isolation conditions of the Local Group from other massive structures. While the observations show that M31 moves towards us on a highly eccentric orbit, the simulation shows that the most common configuration at $z = 0$ has values $v_{\mathrm{rad},\Lambda\mathrm{CDM}} = -65 \pm 5\,\mathrm{km\ s^{-1}}$and $v_{\mathrm{tan},\Lambda\mathrm{CDM}} = 62 \pm 5\ \mathrm{km\ s^{-1}}$.

Using the same absolute values for the uncertainty in the observed velocity components, we find that halos within the preferred ΛCDM values are five times more common than pairs compatible with the observational constraint. The qualitative nature of these results is still valid after a narrower selection on separation and total pair mass. Additionally, pairs with a fraction of tangential to radial velocity $f_{\mathrm{t}} < 0.32$ (similar to observations) represent 8% of the total sample of LG-like pairs. Making an tighter selection to match the observational constraints on the separation and total mass results in zero pairs compatible with observations.

Approximating the LG as two point masses we express the above mentioned results in terms of the orbital angular momentum l_{orb} and the mechanical energy e_{tot} per unit of reduced mass. We find that the uncertainties in the tangential velocity, the square of the norm of the velocity and the total mass in the LG are less constraining on the number of simulated pairs that are consistent with the observations. Nevertheless, in the case of the LG-pair sample that also fulfills the separation and total mass criteria there is a slight tension between simulation and observation. A reduction by a factor of 2 in the observational uncertainty on the radial velocity would clarify this issue.

In the three pairs from constrained simulations we find kinematics dominated by radial velocities. However their velocity components differ from the observational constraints and their mechanical energy and orbital angular momentum are in broad concordance with observations. There is only one pair that fullfills all the separation, total mass constraints and matches the most probable value for the dimensionless spin parameter λ inferred from observations.

The λ spin parameter is itself a useful instrument to gauge the dynamical state of pairs. Reduced uncertainties in masses, distances and velocities can be included to produce an updated estimate for this parameter. This will immedialtly improve the statistical comparison between our Local Group and the expectations from ΛCDM.

In this Letter we have shown that LG-like pairs in ΛCDM show prefered values for their relative velocities, angular momentum and total mechanical energy. The values for the orbital angular momentum and energy, merged into the λ spin parameter, are in mild disagreement with the observational constraints. However, there is a strong tension with the precise values for the radial and tangential velocities.

Under the approximation of consevartion of the orbital angular momentum and mechanical energy, we see that an agreement in the total angular momentum and energy and a marked difference with the precise balance between today's radial and tangential velocities could only be explained if the initial conditions for the formation of the Local Group are special in comparison to the initial conditions of any other pair of dark matter halos in the ΛCDM cosmology. This opens a new window into the question of how unique, if at all, is the LG in a cosmological context. This will continue to be studies within the CLUES framework.

ACKNOWLEDGMENTS

JEF-R acknowledges financial support from the Vicerrectoría de Investigaciones at Universidad de los Andes through its *Fondo de Apoyo a Profesores Asistentes* and the Peter and Patricia Gruber Foundation through its fellowship administered by the International Astronomical Union. JEF-R also acknowledges early discussions with Alejandro García that motivated this work. YH has been supported by the ISF (1013/12)

The data and source code and instructions to replicate the results of this paper can be found as a github repository https://github.com/forero/LG_Kinematics/. Thanks to the IPython community (Pérez & Granger 2007). Thanks to Jessica Kirkpatrick for releasing her Python code to make nice plots of 2D histograms.

The MultiDark Database used in this paper was constructed as part of the activities of the German Astrophysical Virtual Observatory as result of a collaboration between the Leibniz-Institute for Astrophysics Potsdam (AIP) and the Spanish MultiDark Consolider Project CSD2009-00064. The Bolshoi simulation was run on the NASA's Pleiades supercomputer at the NASA Ames Research Center.

REFERENCES

Besla, G., Kallivayalil, N., Hernquist, L., Robertson, B., Cox, T. J., van der Marel, R. P., & Alcock, C. 2007, ApJ, 668, 949
Busha, M. T., Marshall, P. J., Wechsler, R. H., Klypin, A., & Primack, J. 2011, ApJ, 743, 40
Forero-Romero, J. E., Hoffman, Y., Yepes, G., Gottlöber, S., Piontek, R., Klypin, A., & Steinmetz, M. 2011, MNRAS, 417, 1434
Fouquet, S., Hammer, F., Yang, Y., Puech, M., & Flores, H. 2012, MNRAS, 427, 1769
Freeman, K., & Bland-Hawthorn, J. 2002, ARA&A, 40, 487
Gottloeber, S., Hoffman, Y., & Yepes, G. 2010, ArXiv e-prints
Jarosik, N., Bennett, C. L., Dunkley, J., Gold, B., Greason, M. R., Halpern, M., Hill, R. S., Hinshaw, G., Kogut, A., Komatsu, E., Larson, D., Limon, M., Meyer, S. S., Nolta, M. R., Odegard, N., Page, L., Smith, K. M., Spergel, D. N., Tucker, G. S., Weiland, J. L., Wollack, E., & Wright, E. L. 2011, ApJS, 192, 14
Karachentsev, I. D., Karachentseva, V. E., Huchtmeier, W. K., & Makarov, D. I. 2004, AJ, 127, 2031
Kazantzidis, S., Bullock, J. S., Zentner, A. R., Kravtsov, A. V., & Moustakas, L. A. 2008, ApJ, 688, 254
Klypin, A., Gottlöber, S., Kravtsov, A. V., & Khokhlov, A. M. 1999a, ApJ, 516, 530
Klypin, A., Kravtsov, A. V., Valenzuela, O., & Prada, F. 1999b, ApJ, 522, 82
Klypin, A. A., Trujillo-Gomez, S., & Primack, J. 2011, ApJ, 740, 102
Knebe, A., Libeskind, N. I., Doumler, T., Yepes, G., Gottlöber, S., & Hoffman, Y. 2011, MNRAS, 417, L56
Liu, L., Gerke, B. F., Wechsler, R. H., Behroozi, P. S., & Busha, M. T. 2011, ApJ, 733, 62

McConnachie, A. W., Irwin, M. J., Ibata, R. A., Dubinski, J., Widrow, L. M., Martin, N. F., Côté, P., Dotter, A. L., Navarro, J. F., Ferguson, A. M. N., Puzia, T. H., Lewis, G. F., Babul, A., Barmby, P., Bienaymé, O., Chapman, S. C., Cockcroft, R., Collins, M. L. M., Fardal, M. A., Harris, W. E., Huxor, A., Mackey, A. D., Peñarrubia, J., Rich, R. M., Richer, H. B., Siebert, A., Tanvir, N., Valls-Gabaud, D., & Venn, K. A. 2009, Nature, 461, 66

Moore, B., Ghigna, S., Governato, F., Lake, G., Quinn, T., Stadel, J., & Tozzi, P. 1999, ApJ, 524, L19

Peebles, P. J. E. 1971, A&A, 11, 377

Peebles, P. J. E., & Nusser, A. 2010, Nature, 465, 565

Pérez, F., & Granger, B. E. 2007, Comput. Sci. Eng., 9, 21

Purcell, C. W., & Zentner, A. R. 2012, JCAP, 12, 7

Ribas, I., Jordi, C., Vilardell, F., Fitzpatrick, E. L., Hilditch, R. W., & Guinan, E. F. 2005, ApJ, 635, L37

Riebe, K., Partl, A. M., Enke, H., Forero-Romero, J., Gottloeber, S., Klypin, A., Lemson, G., Prada, F., Primack, J. R., Steinmetz, M., & Turchaninov, V. 2011, ArXiv e-prints

Teyssier, M., Johnston, K. V., & Kuhlen, M. 2012, MNRAS, 426, 1808

Tikhonov, A. V., & Klypin, A. 2009, MNRAS, 395, 1915

Tollerud, E. J., Boylan-Kolchin, M., Barton, E. J., Bullock, J. S., & Trinh, C. Q. 2011, ApJ, 738, 102

van der Marel, R. P., Fardal, M., Besla, G., Beaton, R. L., Sohn, S. T., Anderson, J., Brown, T., & Guhathakurta, P. 2012, ApJ, 753, 8

van der Marel, R. P., & Guhathakurta, P. 2008, ApJ, 678, 187